applied sciences

MDPI

Article

Heterocyclic Nitrogen Compounds as Potential PDE4B Inhibitors in Activated Macrophages

Simona Todisco [1], Vittoria Infantino [1], Anna Caruso [1,2,*], Anna Santarsiero [1], Paolo Convertini [1], Hussein El-Kashef [3,4], Federica Giuzio [5,6], Maria Stefania Sinicropi [2] and Carmela Saturnino [1]

[1] Department of Science, University of Basilicata, Viale dell'Ateneo Lucano 10, 85100 Potenza, Italy; simona.todisco@unibas.it (S.T.); vittoria.infantino@unibas.it (V.I.); anna.santarsiero@unibas.it (A.S.); paolo.convertini@gmail.com (P.C.); carmela.saturnino@unibas.it (C.S.)
[2] Department of Pharmacy, Health and Nutritional Sciences, University of Calabria, 87036 Arcavacata di Rende, Italy; s.sinicropi@unical.it
[3] Faculty of Science, Assiut University, Assiut 71516, Egypt; elkashef@aun.edu.eg
[4] Faculty of Pharmacy, Sphinx University, New Assiut 71515, Egypt
[5] U.O.C. Primary Care and Territorial Health, Social and Health Department, State Hospital, 47893 San Marino, San Marino; federica.giuzio@unibas.it
[6] Spinoff TNcKILLERS s.r.l., University of Basilicata, 85100 Potenza, Italy
* Correspondence: anna.caruso@unical.it or anna.caruso@unibas.it

Abstract: Cyclic-nucleotide phosphodiesterases (PDEs) represent a superfamily of enzymes playing a pivotal role in cell signaling by controlling cAMP and cGMP levels in response to receptor activation. PDE activity and expression are linked to many diseases including inflammatory diseases. In light of their specific biochemical properties, PDE inhibition has attracted the interest of several researrs In this context, PDE4 inhibition induces anti-inflammatory effects. Piclamilast and rolipram, well-known PDE4 inhibitors, are endowed with common side effects. The selective phosphodiesterase 4B (PDE4B) inhibitors could be a promising approach to overcome these side effects. In the present study, six potential PDE4B inhibitors have been investigated. Through this study, we identified three PDE4B inhibitors in human macrophages activated by lipopolysaccharide. Interestingly, two of them reduced reactive oxygen species production in pro-inflammatory macrophages.

Keywords: indole; carbazole; purine; PDE4B; inhibitors; macrophage activation; inflammation; reactive oxygen species

Citation: Todisco, S.; Infantino, V.; Caruso, A.; Santarsiero, A.; Convertini, P.; El-Kashef, H.; Giuzio, F.; Sinicropi, M.S.; Saturnino, C. Heterocyclic Nitrogen Compounds as Potential PDE4B Inhibitors in Activated Macrophages. *Appl. Sci.* **2024**, *14*, 6747. https://doi.org/10.3390/app14156747

Academic Editor: Fabrizio Carta

Received: 26 June 2024
Revised: 27 July 2024
Accepted: 1 August 2024
Published: 2 August 2024

1. Introduction

Cyclic-nucleotide phosphodiesterases (PDEs) are found in all organisms and classified into three classes I, II, and III. These enzymes catalyze the hydrolysis of cyclic adenosine 3′,5′-monophosphate (cAMP) and cyclic guanosine 3′,5′-monophosphate (cGMP) to adenosine 5′-monophosphate (AMP) and guanosine 5′-monophosphate (GMP), respectively, to regulate the cellular levels of such important secondary messengers responding to various stimuli in different physiological conditions. In humans, twenty-one PDE genes encode about 100 isoforms of PDEs classified into eleven families (PDE1 to PDE11) with a specific tissue distribution and cellular localization [1]. Certain diseases, including cardiovascular disease, neurodegeneration, and inflammatory diseases, are associated with malfunctions in specific types of PDEs. By considering their specific biochemical properties, transcriptional regulation, and tissue expression, the inhibition of PDEs has attracted the interest of many researchers. Many selective inhibitors of PDEs are identified as anti-depressants, anti-thrombotics, and anti-asthmatics agents [2], and as a treatment for male erectile dysfunction [3].

The cAMP PDEs are sensitive to the competitive inhibitors rolipram and piclamilast (Figure 1), and they have shown functional properties related to inflammatory diseases [4].

Indeed, PDE4 inhibitors are a large group of molecules with anti-inflammatory activity used for the treatment of chronic obstructive pulmonary disease, rheumatoid arthritis, type 2 diabetes, septic shock, and atopic dermatitis [1].

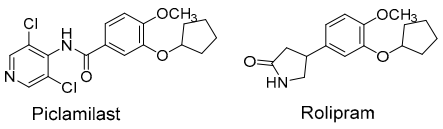

Figure 1. Structures of Piclamilast and Rolipram.

PDE4s include subfamily genes PDE4A-D expressed in immune and inflammatory cells, including T cells, B cells, neutrophils, dendritic cells, monocytes, and macrophages. The isoform PDE4B is upregulated early after stimulation and was found to be induced in monocytes activated by lipopolysaccharide (LPS) [5]. Furthermore, PDE4B was the only isoform expressed in LPS-stimulated mice macrophages [6]. This induction is characterized by an increase in inflammatory mediators such as reactive oxygen species (ROS), and interaction with inflammatory signal proteins like NF-E2-related factor 2 (Nrf2) or Tumor Necrosis Factor α (TNF-α) [7]. Moreover, it was demonstrated that in PDE4B null mice, LPS-stimulated leukocytes are characterized by low levels of TNF-α [8]. Finally, the gene promoter analysis showed that the PDE4B promoter contains sequence motifs to NF-kB, a master transcription factor of macrophages, which are involved in LPS activation and the inflammatory response [9]. Recently, it was demonstrated that macrophages, the main actors of innate immunity [10,11], regulate their response by metabolic rewiring [12] through the production of mediators of inflammation, and by regulating gene expression [13–15] for an immunometabolic response. This metabolic rewiring in LPS-stimulated macrophages is characterized by the activation of the citrate pathway [16], which supports the synthesis of ROS, nitric oxide (NO), and prostaglandins, and contributes to histone acetylation [17]. In light of the involvement of PDE4B in the inflammatory response, together with its activation in LPS-stimulated macrophages and its role as a regulator of cAMP protein kinase A (PKA), the central regulator of many cellular and metabolic processes, the research of new more selective inhibitors of PDE4B takes on importance.

The compounds that we have chosen for this study are the indoles (**1** and **2**), the purines (**3** and **4**), and the carbazoles (**5** and **6**). As it is well known, these classes of compounds were widely studied for their anticancer, antidiabetic, antiviral, antioxidant, anti-inflammatory properties, etc. [18–22]. For this reason, new PDE4B potential inhibitors (**1**–**6**, Figure 2) have been synthesized as reported in Schemes 1–3 and biologically tested. Three of these compounds (**2**, **4**, **6**), in some respects, have been previously studied by our research group [20].

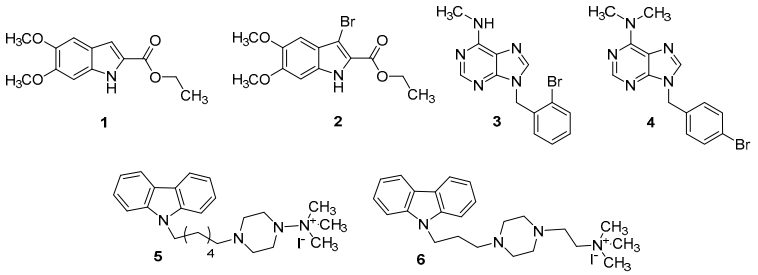

Figure 2. Structure of indole-carboxylates (**1** and **2**), bromobenzyl-purin-amines (**3** and **4**), and quaternary ammonium iodide derivatives (**5** and **6**).

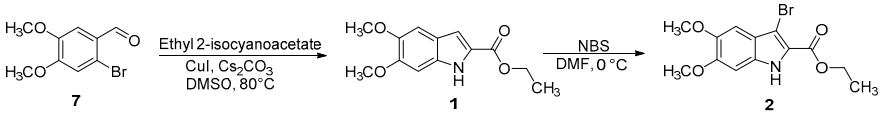

Scheme 1. Synthetic route for the preparation of compounds **1** and **2**.

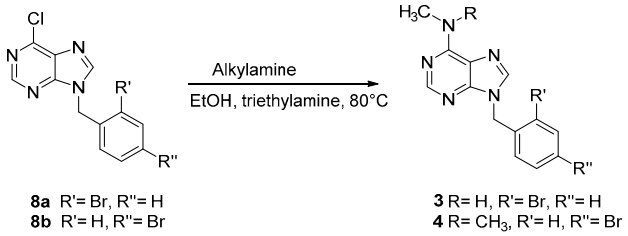

Scheme 2. Synthetic route for the preparation of compounds **3** and **4**.

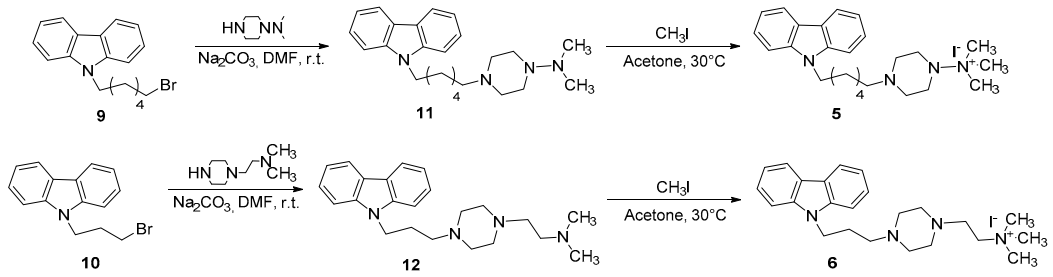

Scheme 3. Synthetic route for the preparation of compounds **5** and **6**.

2. Materials and Methods

2.1. Chemistry

Commercial reagents were purchased from Aldrich, Acros Organics, and Alfa Aesar and used without additional purification. Melting points were determined on a Kofler melting point apparatus Mass spectra were taken on a JEOL JMS GCMate spectrometer (JEOL, Tokyo, Japan) at an ionizing potential of 70 eV (EI) or were performed using a spectrometer LC-MS Waters alliance 2695 (ESI+) (Waters Corporation, Milford, MA, USA) or ESI mass spectrometer Finnigan LCQ Advantage max (International Equipment Trading Ltd., Mundelein, IL, USA). ^{1}H-NMR (300 MHz) and ^{13}C-NMR (75 MHz) were recorded on a Bruker Avance 300 MHz spectrometer (Bruker, Billerica, MA, USA). Chemical shifts were expressed in parts per million downfield from tetramethylsilane as an internal standard. The compounds used in this study were synthesized according to the literature. Ethyl 5,6-dimethoxy-1*H*-indole-2-carboxylate (**1**) and ethyl 3-bromo-5,6-dimethoxy-1*H*-indole-2-carboxylate (**2**) were prepared as shown in Scheme 1 [23,24]. The two derivatives 9-(2-bromobenzyl)-*N*-methyl-9*H*-purin-6-amine (**3**) and 9-(4-bromobenzyl)-*N*,*N*-dimethyl-9*H*-purin-6-amine (**4**) were synthesized according to Scheme 2 [25]. Finally, the two carbazole derivatives 4-(6-(9*H*-carbazol-9-yl)hexyl)-*N*,*N*,*N*-trimethylpiperazin-1-ammonium iodide (**5**) and 2-(4-((9*H*-carbazol-9-yl)propyl)piperazin-1-yl)-*N*,*N*,*N*-trimethylethanammonium iodide (**6**) were synthesized, using our previous methodology [19], from the carbazoles **9** and **10**, respectively (Scheme 3).

2.1.1. Ethyl 5,6-Dimethoxy-1H-indole-2-carboxylate (**1**)

A mixture of 2-bromo-4,5-dimethoxybenzaldehyde (**7**) (7.0 mmol), ethyl 2-isocyanoacetate (7.0 mmol), cesium carbonate (1.0 mmol) and copper(I) iodide (0.14 mmol) in DMSO (20 mL) was heated at 80 °C under stirring for 12 h. The reaction mixture was then allowed to cool to room temperature and diluted with ice-cold water (20 mL). The resulting mixture was extracted with dichloromethane (3 × 20 mL). The combined organic layers were washed with brine, dried over anhydrous Na_2SO_4 and concentrated under vacuum. The residue obtained was chromatographed on silica gel column using *n*-hexane/EtOAc (1:1) as an eluent to give the desired indole **1** as a white solid, yield (80%), mp: 176 °C. ^{1}H-NMR (300 MHz, $CDCl_3$): δ = 9.42 (bs, 1H, NH), 7.70 (d, 1H, Ar), 7.40 (d, 1H, Ar), 6.80 (s, 1H, Ar), 4.60–4.30 (m, 2H, CH_2), 3.94 (s, 3H, OCH_3), 3.89 (s, 3H, OCH_3), 1.48 (t, 3H, CH_3); ^{13}C NMR (75 MHz, $CDCl_3$): δ = 159.19, 150.76, 146.34, 130.96, 125.15, 123.65, 110.81, 104.54, 99.46, 60.66, 55.22, 16.76; MS (EI) *m*/*z* (%): 250 [M^+,1]; Anal. calcd for $C_{13}H_{15}NO_4$: C 62.64, H 6.07, N 5.62, found: C 62.62, H 6.09, N 5.65.

2.1.2. Ethyl 3-Bromo-5,6-dimethoxy-1H-indole-2-carboxylate (**2**)

To a cold solution (0 °C) of the indole **1** (5.0 mmol) in DMF (5 mL), a solution (0 °C) of NBS (5.0 mmol) in DMF (5 mL) was slowly added. The resulting reaction mixture was stirred at the same temperature (0 °C) for 2 h. Stirring was continued at room temperature for 10 h. Water (50 mL) was then added, and the resulting mixture was extracted with ethyl acetate (3 × 20 mL). The combined organic layers were washed with brine, dried over anhydrous Na_2SO_4, and concentrated under vacuum. The residue obtained was chromatographed on silica gel column using petroleum ether/EtOAc (1:1) as an eluent to give the desired indole **2** as a white solid (76% yield); mp: 179 °C. ^{1}H NMR (300 MHz, $CDCl_3$): δ = 9.50 (bs, 1H, NH), 7.71 (d, 1H, Ar), 6.88 (s, 1H, Ar), 4.58–4.27 (m, 2H, CH_2), 3.93 (s, 3H, OCH_3), 3.85 (s, 3H, OCH_3), 1.48 (t, 3H, CH_3); ^{13}C NMR (75 MHz, $CDCl_3$): δ = 160.19, 151.78, 147.32, 130.98, 125.25, 124.65, 110.80, 105.54, 99.54, 60.68, 55.43, 16.89; MS (EI) *m*/*z* (%): 329 [M^+,1]; Anal. calcd for $C_{13}H_{14}BrNO_4$: C 47.58, H 4.30, N 4.27, found: C 47.60, H 4.33, N 4.31.

2.1.3. General Procedure for the Synthesis of Compounds **3** and **4**

To a solution of **8a** or **8b** (10 mmol) in absolute ethanol (50 mL), the appropriate amine (13.0 mmol) was added in the presence of triethylamine (0.5 mL). The reaction mixture was heated under reflux for 3 h. Then, it was concentrated and left to cool. The solid product obtained was filtered off and crystallized from ethanol.

9-(2-Bromobenzyl)-*N*-methyl-9*H*-purin-6-amine (**3**): white solid (58% yield); m.p. 260 °C. ^{1}H-NMR (300 MHz, DMSO-d_6): δ = 8.18 (s, 1H, *purine*), 7.80 (d, 1H, *purine*), 7.50–7.12 (m, 4H, *Ar*), 5.47–5.38 (m, 2H, CH_2), 3.95 (br, 1H, N*H*); 2.75 (s, 3H, CH_3); ^{13}C NMR (75 MHz, DMSO-d_6): δ = 154.82, 152.19, 150.78, 146.32, 140.98, 135.05, 127.60, 120.70, 52.65, 28.01; MS (ESI^+): 318 $[M+1]^+$; Anal. calcd. for $C_{13}H_{12}BrN_5$: C 49.07, H 3.80, N 22.01. Found: C 49.10; H 3.78, N 22.03.

9-(4-Bromobenzyl)-*N*,*N*-dimethyl-9*H*-purin-6-amine (**4**): white solid (68% yield); m.p. 268 °C. ^{1}H-NMR (300 MHz, DMSO-d_6): δ = 8.20 (s, 1H, *purine*), 7.81–7.76 (m, 1H, *purine*, 2H *Ar*), 7.69–7.07 (m, 4H, *Ar*), 5.46–5.35 (m, 2H, CH_2), 3.75 (s, 6H, 2CH_3); ^{13}C NMR (75 MHz, DMSO-d_6): δ = 157.32, 152.29, 149.79, 145.78, 136.05, 131.45, 120.60, 119.76, 50.45, 39.01; MS (ESI^+): 332 $[M+1]^+$; Anal. calcd. for $C_{14}H_{14}BrN_5$: C 50.62, H 4.25, N 21.08. Found: C 50.60; H 4.28, N 21.11.

2.1.4. General Procedure for the Synthesis of Compounds **5** and **6**

Methyl iodide (80 mmol, 5 mL) was added to a solution of **11** or **12** (1 mmol) in acetone (10 mL), and the reaction mixture was heated at 30 °C for 1 h. After evaporation of the solvent, the solid residue was recrystallized from methanol.

4-(6-(9*H*-carbazol-9-yl)hexyl)-*N*,*N*,*N*-trimethylpiperazin-1-ammonium iodide (**5**): white solid (60% yield); mp: 110 °C. ^{1}H NMR (300 MHz, $CDCl_3$): δ = 8.32 (d, 1H, *Ar*), 8.08 (d, 1H, *Ar*), 7.73 (d, 1H, *Ar*), 7.65 (d, 1H, *Ar*), 7.43–7.29 (m, 4H, *Ar*), 3.90 (t, 2H, CH_2N), 3.10 (t, 2H, NCH_2), 2.90 (s, 9H, 3CH_3), 2.70–2.46 (m, 8H, CH_2-piperazine), 1.70–1.63 (m, 2H, CH_2), 1.40–1.36 (m, 2H, CH_2), 1.29–1.24 (m, 4H, 2CH_2); ^{13}C NMR (75 MHz, $CDCl_3$): δ = 133.99, 122.98, 121.15, 119.82, 119.36, 56.76, 54.22, 53.73, 53.43, 50.10, 30.02, 28.10, 27.30; MS (EI) *m*/*z* (%): 393 [M^+ -I]; Anal. calcd for $C_{25}H_{37}IN_4$: C 57.69, H 7.17, N 10.76, found: C 57.71, H 7.19, N 10.80.

2-(4-((9*H*-carbazol-9-yl)propyl)piperazin-1-yl)-*N*,*N*,*N*-trimethylethanammonium iodide (**6**): white solid (65% yield); mp: 113 °C. ^{1}H NMR (300 MHz, $CDCl_3$): δ = 8.34 (d, 1H, *Ar*), 8.00 (d, 1H, *Ar*), 7.70 (d, 1H, *Ar*), 7.60 (d, 1H, *Ar*), 7.46–7.27 (m, 4H, *Ar*), 2.55–2.50 (m, 4H, 2CH_2), 2.49–2.45 (m, 8H, CH_2-piperazine), 2.35 (t, 2H, CH_2N), 2.34–2.29 (m, 4H, 2CH_2), 2.28 (s, 9H, 3CH_3); ^{13}C NMR (75 MHz, $CDCl_3$): δ = 132.99, 121.97, 120.15, 119.79, 119.41, 111.20, 65.01, 60.30, 54.46, 53.88, 53.73, 52.10, 46.37, 28.12, 26.30; MS (EI) *m*/*z* (%): 379 [M^+ -I]; Anal. calcd for $C_{24}H_{35}IN_4$: C 56.92, H 6.97, N 11.06, found: C 56.93, H 6.95, N 11.04.

2.1.5. General Procedure for the Synthesis of Compounds **11** and **12**

To a solution of the appropriate piperazine (1-(*N*,*N*-dimethylamino) piperazine or 1-(2-*N*,*N*-dimethylaminoethyl)piperazine) (l.35 mmol) and Na_2CO_3 (2.7 mmol) in DMF (10 mL), a solution of *N*-bromoalkyl-substituted carbazole (**9** or **10**) (1.35 mmol) in DMF (10 mL) was added at r.t. The reaction mixture was stirred for 20 h. After, the mixture was poured onto ice-cold water and extracted with chloroform (3 × 50 mL). The organic layer was washed with brine, dried over anhydrous $MgSO_4$, and evaporated under reduced pressure. The residue obtained was chromatographed on silica gel column using *n*-hexane/EtOAc (1:1).

9*H*-9-(6-(4-*N*,*N*-dimethylaminopiperazin-1-yl)hexyl)carbazole (**11**): white solid (65% yield); mp: 107 °C. ^{1}H NMR (300 MHz, $CDCl_3$): δ = 8.32 (d, 1H, *Ar*), 8.09 (d, 1H, *Ar*), 7.73 (d, 1H, *Ar*), 7.68 (d, 1H, *Ar*), 7.42–7.29 (m, 4H, *Ar*), 3.90 (t, 2H, CH_2N), 3.10 (t, 2H, NCH_2), 2.91 (s, 6H, 2CH_3), 2.71–2.46 (m, 8H, CH_2-piperazine), 1.72–1.65 (m, 2H, CH_2), 1.40–1.36 (m, 2H, CH_2), 1.28–1.24 (m, 4H, 2CH_2); ^{13}C NMR (75 MHz, $CDCl_3$): δ = 134.19, 122.95, 122.15, 119.81, 119.46, 56.66, 54.22, 53.73, 53.41, 40.10, 30.12, 28.10, 27.32; MS (ESI^+): 379 $[M+1]^+$; Anal. calcd for $C_{24}H_{34}N_4$: C 76.15, H 9.05, N 14.80, found: C 76.12, H 9.07, N 14.82.

2-(4-((9*H*-carbazol-9-yl)propyl)piperazin-1-yl)-*N*,*N*-dimethylethanamine (**12**): this was obtained as a white powder (70% yield); mp: 109 °C. ^{1}H NMR (300 MHz, $CDCl_3$): δ = 8.34 (d, 1H, *Ar*), 8.00 (d, 1H, *Ar*), 7.70 (d, 1H, *Ar*), 7.60 (d, 1H, *Ar*), 7.46–7.27 (m, 4H, *Ar*), 2.55–2.50 (m, 4H, 2CH_2), 2.49–2.45 (m, 8H, CH_2-piperazine), 2.35 (t, 2H, CH_2N), 2.34–2.29 (m, 4H, 2CH_2), 2.26 (s, 6H, 2CH_3); ^{13}C NMR (75 MHz, $CDCl_3$): δ = 139.49, 125.68, 123.39, 121.37, 119.30, 108.51, 53.54, 52.10, 51.67, 51.59, 50.00, 46.44, 43.35, 29.90; MS (ESI^+): 365 $[M+1]^+$; Anal. calcd for $C_{23}H_{32}N_4$: C 75.78, H 8.85, N 15.37, found: C 75.77, H 8.87, N 15.39.

2.2. Human PDE4B ELISA Assay

The synthesized molecules (**1**–**6**) were dissolved in 100% dimethyl sulfoxide (DMSO) (Sigma-Aldrich, St Louis, MO, USA) to make stock solutions, and then sterile water was used for dilutions. The effect of the prepared compounds was evaluated by using the Human PDE4B (cAMP-specific 3′,5′-cyclic phosphodiesterase 4B) ELISA Kit (Code number: HUEB0664 Creative Diagnostics, Shirley, NY, USA), a quantitative sandwich enzyme immunoassay, following the manufacturer's recommendations. The human PDE4B (5 ng/mL) or the cell extract (350 μg/mL cell protein) was added to a 96-well plate. A biotinylated antibody specific for PDE4B was dispensed, either with or without compounds **1**–**6** at concentrations of 100 nM or 10 μM. Following incubation and washing, Streptavidin-horseradish peroxidase (Streptavidin-HRP) was added to the wells. The plate was incubated and washed again to remove unbound reagents. The interaction between Streptavidin-HRP and the biotinylated antibody, in the presence of 3,3′,5,5′-tetramethylbenzidine (TMB) substrate, produced a blue-colored reaction product. The reaction was stopped by a stop solution, turning the color to yellow. The intensity of coloration was related to the interaction between human PDE4B and the synthesized molecules. The results were reported as a percentage of the controls, indicating the compounds' ability to inhibit antibody binding.

2.3. Isolation of Human PBMCs and Differentiation of PBMC-Derived Macrophages

Peripheral blood mononuclear cells (PBMCs) were isolated from whole blood derived from anonymous healthy human donors. Informed consent was obtained from all participants in the study. The research was carried out in accordance with the principles outlined in the Declaration of Helsinki and following the approved procedures of the local Italian Committee on Human Research (REF. TS/CEUR-CET/CEL n.20230044811—3 November 2023). Heparinized blood was mixed with Hanks' balanced salt solution (HBSS, Thermo Fisher Scientific, Grand Island, NY, USA) at 1:2 (*v*/*v*) ratio. This mixture was then carefully layered over Histopaque-1077 (Sigma-Aldrich). The samples were centrifuged at 1000× *g* for 15 min at room temperature. After centrifugation, the mononuclear cell layer was recovered and washed twice in HBSS. PBMCs were cultured in Roswell Park Memorial Institute (RPMI) 1640 medium (Thermo Fisher Scientific) supplemented with 10% fetal bovine serum, 2 mM L-glutamine, 100 U/mL penicillin, 100 μg/mL streptomycin, and

100 ng/mL recombinant human M-CSF (Cell Guidance Systems, St. Louis, MO, USA) at 37 °C in a humidified chamber of 5% CO_2.

2.4. Cell Viability Assay

Cell viability was determined by CellTiter-Glo® 2.0 Cell Viability Assay (Promega, Madison, WI, USA), as previously described [26]. Briefly, PBMC-derived human macrophages (8×10^3 cells/well in a 96-well plate) were treated with **1**–**6** molecules at increasing concentrations (100 nM, 10 µM, and 1 mM) while the control group received DMSO equivalent to the maximum < 0.1% solvent used in the experimental settings. At the end of the 72 h treatment, 100 µL of CellTiter-Glo® 2.0 Reagent (Promega, Madison, WI, USA) was added, and luminescence was recorded by GloMax® Discover Microplate Reader (Promega).

2.5. Reactive Oxygen Species (ROS) Detection

For evaluation of ROS, human macrophages (6×10^4 cells/well in a 12-well plate) were treated with 100 nM or 10 µM of the synthetic molecules, while the control group was administered with DMSO equivalent to the maximum < 0.1% solvent used in the experimental settings. Following 1 h, cells were triggered by 1 µg/mL lipopolysaccharide (LPS) from *Salmonella enterica* serotype Typhimurium (Sigma-Aldrich). ROS were quantified after 24 h of LPS-stimulation by using 6-carboxy-2′,7′-dichlorodihydrofluorescein diacetate (DCF-DA, Thermo Fisher Scientific). Briefly, the cells were collected in 1.5 mL tubes at the end of treatments and counted. After 5 min of centrifugation at 8600× *g*, the cell pellet was resuspended in Phosphate Buffer Saline (PBS) to have 10^5 cells/100 µL. Then, 10 µM DCF-DA was added. After 30 min of incubation at 37 °C in the dark, a 100 µL aliquot of the sample was dispensed into three separate groups of wells on a black microtiter plate and the fluorescence was revealed by GloMax® Discover Microplate Reader (Promega).

2.6. Statistical Analysis

Statistical analyses were conducted using GraphPad Prism software version number 8.0.2. Results are expressed as the mean ± standard deviation (SD) from three independent experiments, each performed in triplicate. Data were analyzed by one-way ANOVA followed by Dunnett's or Tukey's multiple comparison tests. The specific statistical methods used for each experiment are detailed in the figure legends. In the figures, asterisks indicate statistical significance (* $p < 0.05$; ** $p < 0.01$; and *** $p < 0.001$). When Tukey's test was used, different letters were employed to indicate significant differences between treatments at $p < 0.05$.

3. Results and Discussion

3.1. Chemistry

Ethyl 5,6-dimethoxy-1*H*-indole-2-carboxylate (**1**) and ethyl 3-bromo-5,6-dimethoxy-1*H*-indole-2-carboxylate (**2**) were prepared as reported in Scheme 1. The indole **1** was obtained by a copper-catalyzed domino reaction of 2-bromo-4,5-dimethoxybenzaldehyde (**7**) with ethyl 2-isocyanoacetate, in the presence of copper(I) iodide (CuI) and cesium carbonate (Cs_2CO_3) in dimethyl sulfoxide (DMSO) at 80 °C. Regioselective bromination of **1** using *N*-bromosuccinimide (NBS), in dimethylformamide (DMF) at 0 °C, gave the 3-bromoindole derivative **2** [23,24].

9-(2-Bromobenzyl)-*N*-methyl-9*H*-purin-6-amine (**3**) and 9-(4-bromobenzyl)-*N*,*N*-dimethyl-9*H*-purin-6-amine (**4**) were synthesized as reported in Scheme 2. Derivatives **3** and **4** were obtained from the reaction of corresponding chloropurines **8** with appropriate alkylamines in boiling absolute ethanol in the presence of triethylamine [25].

The 4-(6-(9*H*-carbazol-9-yl)hexyl)-*N*,*N*,*N*-trimethylpiperazin-1-ammonium iodide (**5**) and 2-(4-((9*H*-carbazol-9-yl)propyl)piperazin-1-yl)-*N*,*N*,*N*-trimethylethanammonium iodide (**6**) were synthesized, respectively, from carbazole **9** and **10** in two steps, as shown in Scheme 3. In the first step, *N*-bromoalkylated derivative **9** was reacted with *N*,*N*-dimethylpiperazin-1-amine to give the carbazole derivative **11**. Alternatively, when the

N-bromoalkylated derivative **10** was reacted with 1-[2-(dimethylamino)ethyl]piperazine, the carbazole derivative **12** was obtained. In the second step, the quaternization of compounds **11** and **12** was accomplished using an excess of methyl iodide in acetone, to give the quaternary ammonium iodide derivatives **5**–**6**, respectively [18].

3.2. Human PDE4B Is Affected by Synthetic Molecules **1**–**6**

In order to understand whether the synthesized compounds **1**–**6** could have an effect on human PDE4B function, they were tested by ELISA assay. In Figure 3, the results of ELISA immunoassay for human PDE4B are reported. The intensity of colored product significantly decreased in the presence of 100 nM of both **1** and **3** molecules. When the compounds were used at the concentration of 10 µM, inhibitory activity was obtained after treatment with compounds **1**, **2** or **3**. Molecules **4**–**6** showed no inhibitory effect on PDE4B either at 100 nM or 10 µM. Indeed, even at the highest concentration, they lead to an increase in PDE4B. Notably, when the same experiments were performed using each potential inhibitor alone (without PDE4B), we did not observe any signals. These preliminary results indicated that compounds **1**–**3** bind to human PDE4B by impacting the interaction with the specific antibody and potentially by affecting PDE4B activity.

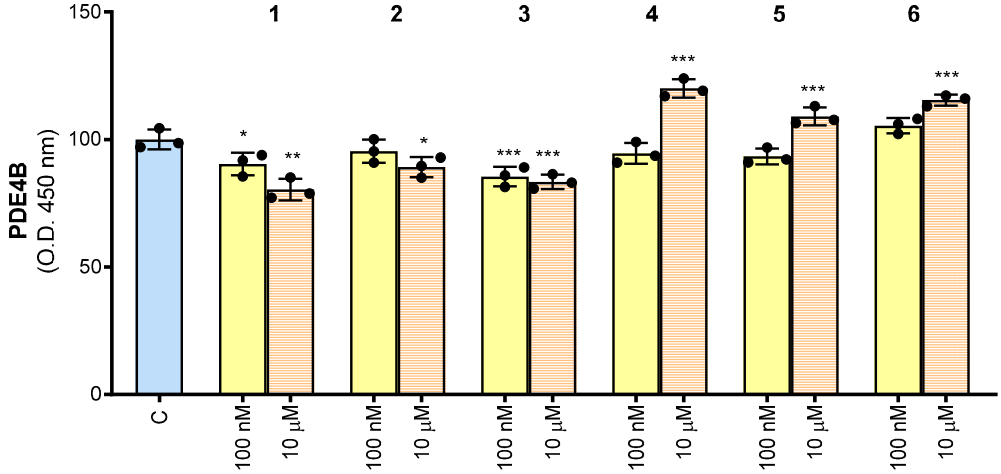

Figure 3. Human PDE4B detection using the ELISA assay. Results are expressed as a percentage of unstimulated control cells (C, set at 100%). Mean values ± SD of three independent experiments with four replicates in each. Dots represent the mean values obtained from each experiment. Where indicated, differences were significant according to one-way ANOVA followed by Dunnett's multiple comparison test (* $p < 0.05$; ** $p < 0.01$; *** $p < 0.001$).

3.3. Effect of Molecules **1**–**6** *on Cell Viability*

We next investigated the effect of synthesized compounds **1**–**6** on cell viability. To this end, PBMCs were isolated from the whole blood of healthy human donors and differentiated into macrophages. PBMC-derived macrophages were treated with increasing concentrations of **1**–**6**. More specifically, **1**–**6** were evaluated by testing a wide range of concentrations from 100 nM to 1 mM. We observed that **1** and **5** reduced cell viability by about 10% at 100 nM, although not significantly. Except for **6**, which caused a slight 15% reduction in cell viability, no molecule was toxic at 10 µM. When used at 1 mM, all molecules significantly reduced cell viability by a minimum of 20% (**5**) to a maximum of 65% (**2**) (Figure 4).

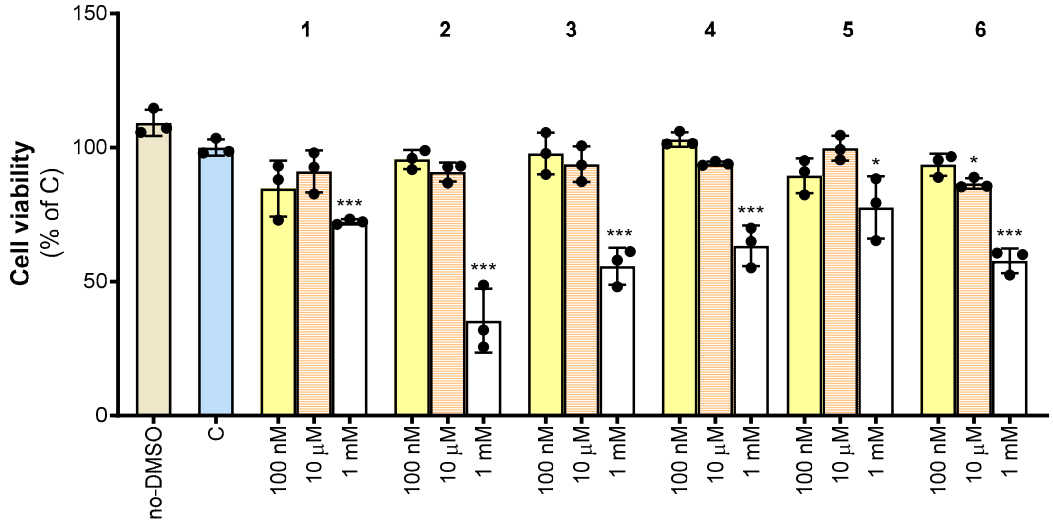

Figure 4. Effect of derivatives **1**–**6** on cell viability. Cell viability was assessed in untreated PBMC-derived macrophages (no-DMSO), or macrophages treated with the vehicle DMSO (C) or synthetic molecules **1**–**6** at the indicated concentrations (100 nM, 10 μM, and 1 mM) after 72 h exposure. Data are expressed as a percentage of C (mean values ± SD) from three independent experiments, each with four replicates. Dots represent the mean values obtained from each experiment. Where indicated, differences were significant according to one-way ANOVA followed by Dunnett's multiple comparison test (* $p < 0.05$; *** $p < 0.001$).

3.4. Compounds **1**–**3** *Affect LPS-Induced PDE4B Response*

After finding that none of the molecules significantly altered PBMC-derived macrophage cell viability at 100 nM and 10 μM, we decided to test these concentrations in the following experiments.

Given that PDE4B is upregulated in response to LPS stimulation leading to increased secretion of ROS inflammatory mediators [27], we investigated the potential effect of synthesized molecules (**1**–**6**) on ROS production in human PBMC-derived macrophages induced by LPS.

In M1 macrophages activated with LPS, there are different sites of ROS production, including NADPH oxidase (NOX), the mitochondrial electron transport chain, lipoxygenase, cyclooxygenases (COX), xanthine oxidase, and monoamine oxidase [28], that regulate the proinflammatory response. The redox balance is essential to restore a physiological condition after an inflammatory response. Since many diseases are characterized by ROS dysregulation, identification of the specific source of ROS as well as its specific inhibitors could be relevant. In this context, NOX and PDE inhibitors are under investigation as treatments for neurological disorders [29,30] and arthritis [1,31], respectively. In our experiments, we observed an approximate 20% increase in ROS levels when macrophages were stimulated with LPS (L, Figure 5A), which is completely abrogated in the presence of hydroxycitrate (HCA), the specific inhibitor of ATP citrate lyase (ACLY), able to decrease ROS levels in M1 macrophages [13].

None of the newly synthesized molecules significantly reduced ROS levels when tested at 100 nM (Figure 5A). However, at 10 μM, **3** reduced ROS to levels comparable to those of unstimulated cells (100.3 ± 3.3% of C), while **2** exhibited an even stronger decrease (87.3 ± 5.3% of C; Figure 5A). Derivatives **1**, **4**, and **6** had no significant effects on ROS levels, whereas **5** even increased ROS secretion compared to LPS-stimulated cells (Figure 5A).

Based on the results obtained, we tested synthetic molecules **1**–**6**, at the concentration of 10 μM, on cell extract from LPS-induced macrophages. Our findings confirmed that PDE4B is activated by LPS treatment. Indeed, an increase in the intensity of the yellow-colored product in LPS-triggered macrophage cell extracts was observed when compared with the control (Figure 5B). Furthermore, a decrease in intensity was observed when

compounds **1**–**3** were added to the cell extracts (Figure 5B), suggesting that these molecules could affect PDE4B activity in human PBMC-derived macrophages activated by LPS.

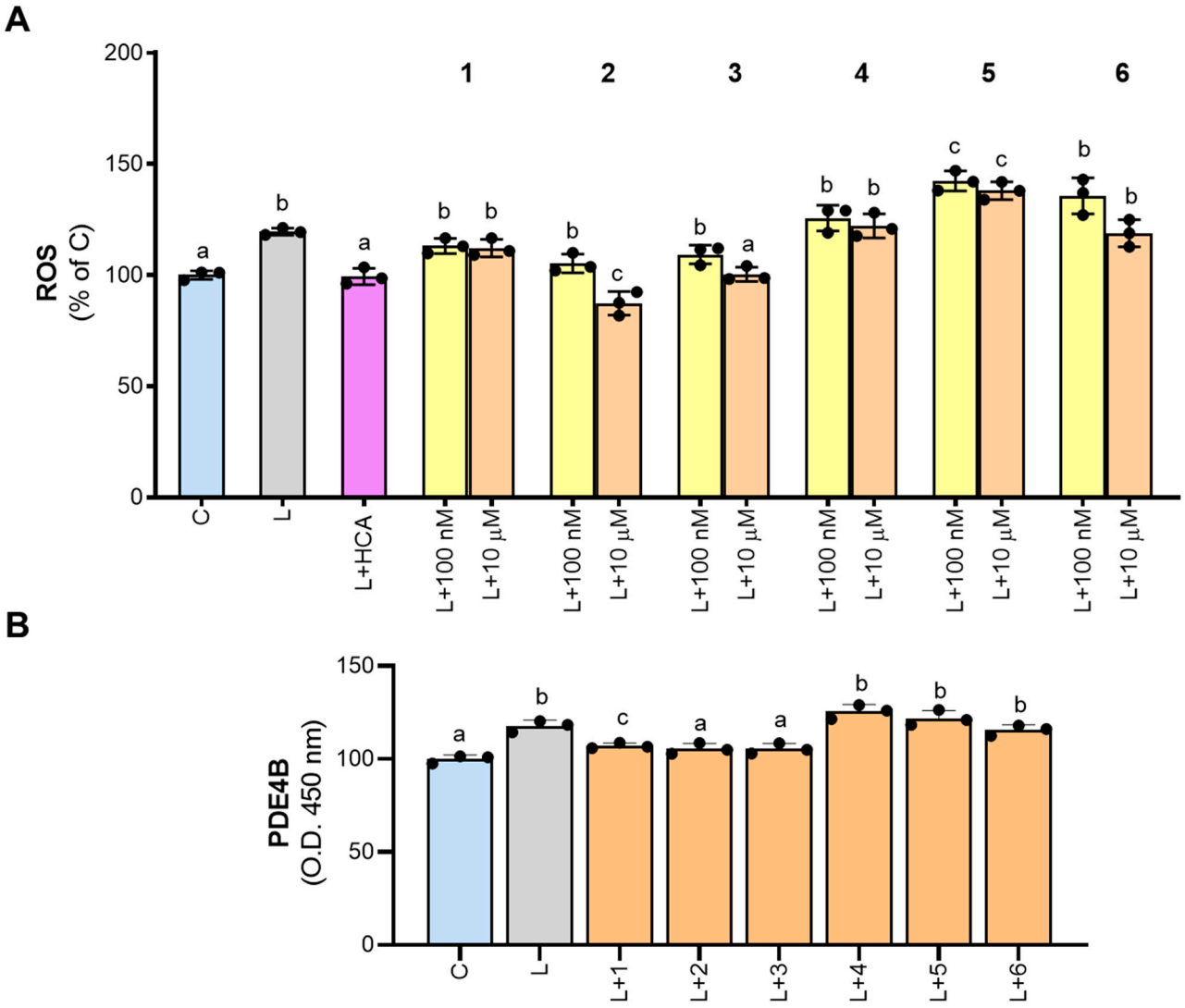

Figure 5. Effect of derivatives **1**–**6** on ROS production and PDE4B inhibition. PBMC-derived macrophages were treated with LPS alone (L) or in combination with 500 µM hydrocitrate (HCA) or molecules **1**–**6**. In panel (**A**), **1**–**6** were tested at both 100 nM and 10 µM concentrations, while in panel (**B**), they were tested only at 10 µM. After 24 h, ROS levels (**A**) and PDE4B (**B**) were quantified. Results are expressed as a percentage of unstimulated control cells (C, set at 100%). Mean values ± SD of three independent experiments with at least three replicates in each are presented. Dots represent the mean values obtained from each experiment. The data were analyzed using one-way ANOVA. For all experiments, the *p*-value was <0.05. Therefore, Tukey's test for multiple comparisons was performed. Different letters (a, b, and c) indicate statistically significant differences among treatments.

In summary, our study of the six molecules (**1**–**6**) suggests that the bicyclic structure is more likely to inhibit the PDE4B activity than a tricyclic one. Molecules containing an indole ring as **1** and **2** or a pyridine ring as **3** showed better inhibitory activity in comparison with those having a carbazole ring system as **5** and **6**. This could be because the larger size of the carbazole system in derivatives **5** and **6** might lead to steric hindrance. This means that the bulky carbazole group could prevent proper interaction with crucial amino acids in the active site, hindering effective binding and potentially causing partial inhibition or even activation (as observed at high concentrations). However, this is not the case with compounds **1**, **2** and **3** that have a slightly smaller structure, such as piclamilast (selective

second generation PDE4 inhibitor). Furthermore, as reported in the literature [20], the molecular docking studies on the active site of PDE4B showed that, in comparison with a carbazole nucleus, a pyridine moiety makes two more bonds on the active site of PDE4B, in particular, a hydrogen bond with S282 and a strong bond with Mg^{2+} (ion present at the catalytic site of PDE4B).

The presence of a bromine atom, especially on the main ring system (compound **2**), seemed beneficial. This is evident when comparing compound **2** (bromine on the indole ring at position 3) with molecule **3** (bromine on the benzyl group).

Molecules **1**–**3** appeared to be more effective in inhibiting PDE4B activity in pro-inflammatory macrophages. Molecules **2** and **3** also significantly reduced ROS levels in human macrophages derived from LPS-induced PBMCs. However, further research is needed to fully understand the biological properties of these potential new PDE4B inhibitors.

4. Conclusions

In conclusion, considering the six molecules that we have studied **1**–**6**, the results showed that inhibitory activity on PDE4B is likely favored by the presence of a bicyclic- rather than a tricyclic system in the compound structure. Therefore, an indole ring, as in derivatives **1**,**2**, or a pyridine nucleus, as in derivative **3**, favored the inhibitory activity. However, a carbazole system (derivatives **5**,**6**) resulted in the opposite effect. The presence of a halogen atom such as bromine is appreciated, especially if it is found as a substituent in the heterocyclic system (compound **2**). This is quite clear upon comparing the inhibitory effect of compound **2**, where the bromine substituent is located at position **3** of the indole ring, with that of compound **3** where the bromine is a substituent on the benzyl group. The three compounds **1**–**3** seem to be better correlated with PDE4B activity in pro-inflammatory macrophages, while compounds **2** and **3** can significantly reduce ROS levels in PBMC-derived human macrophages triggered by LPS. However, future investigations will be important to better biologically characterize the new potential PDE4B inhibitors we have identified.

Author Contributions: Conceptualization, C.S. and F.G.; methodology, A.S., S.T. and A.C.; formal analysis, A.S., P.C. and S.T.; investigation, A.S. and S.T.; resources, V.I., C.S. and M.S.S.; writing—original draft preparation, A.C., A.S., P.C., V.I. and S.T.; writing—review and editing, A.S., V.I. and S.T.; supervision, V.I., A.C. and H.E.-K. All authors have read and agreed to the published version of the manuscript.

Funding: This research received no external funding.

Institutional Review Board Statement: Not applicable.

Informed Consent Statement: Not applicable.

Data Availability Statement: The raw data supporting the conclusions of this article will be made available by the authors on request.

Conflicts of Interest: The authors declare no conflicts of interest.

References

1. Wang, H.; Peng, M.S.; Chen, Y.; Geng, J.; Robinson, H.; Houslay, M.D.; Cai, J.; Ke, H. Structures of the four subfamilies of phosphodiesterase-4 provide insight into the selectivity of their inhibitors. *Biochem. J.* **2007**, *408*, 193–201. [CrossRef]
2. Keravis, T.; Lugnier, C. Cyclic nucleotide phosphodiesterase (PDE) isozymes as targets of the intracellular signalling network: Benefits of PDE inhibitors in various diseases and perspectives for future therapeutic developments. *Br. J. Pharmacol.* **2012**, *165*, 1288–1305. [CrossRef]
3. Francis, S.H.; Morris, G.Z.; Corbin, J.D. Molecular mechanisms that could contribute to prolonged effectiveness of PDE5 inhibitors to improve erectile function. *Int. J. Impot. Res.* **2008**, *20*, 333–342. [CrossRef]
4. Jin, S.L.; Ding, S.L.; Lin, S.C. Phosphodiesterase 4 and its inhibitors in inflammatory diseases. *Chang. Gung Med. J.* **2012**, *35*, 197–210. [CrossRef]

5. Ma, D.; Wu, P.; Egan, R.W.; Billah, M.M.; Wang, P. Phosphodiesterase 4B gene transcription is activated by lipopolysaccharide and inhibited by interleukin-10 in human monocytes. *Mol. Pharmacol.* **1999**, *55*, 50–57. [CrossRef]
6. Jin, S.L.; Lan, L.; Zoudilova, M.; Conti, M. Specific role of phosphodiesterase 4B in lipopolysaccharide-induced signaling in mouse macrophages. *J. Immunol.* **2005**, *175*, 1523–1531. [CrossRef]
7. Dhar, R.; Rana, M.N.; Zhang, L.; Li, Y.; Li, N.; Hu, Z.; Yan, C.; Wang, X.; Zheng, X.; Liu, H.; et al. Phosphodiesterase 4B is required for NLRP3 inflammasome activation by positive feedback with Nrf2 in the early phase of LPS- induced acute lung injury. *Free Radic. Biol. Med.* **2021**, *176*, 378–391. [CrossRef]
8. Jin, S.L.; Conti, M. Induction of the cyclic nucleotide phosphodiesterase PDE4B is essential for LPS-activated TNF-alpha responses. *Proc. Natl. Acad. Sci. USA* **2002**, *99*, 7628–7633. [CrossRef]
9. Iacobazzi, D.; Convertini, P.; Todisco, S.; Santarsiero, A.; Iacobazzi, V.; Infantino, V. New Insights into NF-κB Signaling in Innate Immunity: Focus on Immunometabolic Crosstalks. *Biology* **2023**, *12*, 776. [CrossRef]
10. Mantovani, A.; Sica, A. Macrophages, innate immunity and cancer: Balance, tolerance, and diversity. *Curr. Opin. Immunol.* **2010**, *22*, 231–237. [CrossRef]
11. Netea, M.G.; Nold-Petry, C.A.; Nold, M.F.; Joosten, L.A.; Opitz, B.; van der Meer, J.H.; van de Veerdonk, F.L.; Ferwerda, G.; Heinhuis, B.; Devesa, I.; et al. Differential requirement for the activation of the inflammasome for processing and release of IL-1beta in monocytes and macrophages. *Blood* **2009**, *113*, 2324–2335. [CrossRef]
12. Wang, L.; Wang, D.; Zhang, T.; Ma, Y.; Tong, X.; Fan, H. The role of immunometabolism in macrophage polarization and its impact on acute lung injury/acute respiratory distress syndrome. *Front. Immunol.* **2023**, *14*, 1117548. [CrossRef]
13. Infantino, V.; Pierri, C.L.; Iacobazzi, V. Metabolic Routes in Inflammation: The Citrate Pathway and its Potential as Therapeutic Target. *Curr. Med. Chem.* **2019**, *26*, 7104–7116. [CrossRef]
14. Convertini, P.; Santarsiero, A.; Todisco, S.; Gilio, M.; Palazzo, D.; Pappalardo, I.; Iacobazzi, D.; Frontuto, M.; Infantino, V. ACLY as a modulator of liver cell functions and its role in Metabolic Dysfunction-Associated Steatohepatitis. *J. Transl. Med.* **2023**, *21*, 568. [CrossRef]
15. Netea, M.G.; Joosten, L.A. Master and commander: Epigenetic regulation of macrophages. *Cell Res.* **2016**, *26*, 145–146. [CrossRef]
16. Santarsiero, A.; Onzo, A.; Pascale, R.; Acquavia, M.A.; Coviello, M.; Convertini, P.; Todisco, S.; Marsico, M.; Pifano, C.; Iannece, P.; et al. Hydrosol: Untargeted Metabolomic Analysis and Anti-Inflammatory Activity Mediated by NF-κB and the Citrate Pathway. *Oxidative Med. Cell. Longev.* **2020**, *2020*, 4264815. [CrossRef]
17. Santarsiero, A.; Convertini, P.; Todisco, S.; Pierri, C.L.; De Grassi, A.; Williams, N.C.; Iacobazzi, D.; De Stefano, G.; O'Neill, L.A.J.; Infantino, V. ACLY Nuclear Translocation in Human Macrophages Drives Proinflammatory Gene Expression by NF-κB Acetylation. *Cells* **2021**, *10*, 2962. [CrossRef]
18. Saturnino, C.; Caruso, A.; Iacopetta, D.; Rosano, C.; Ceramella, J.; Muià, N.; Mariconda, A.; Bonomo, M.G.; Ponassi, M.; Rosace, G.; et al. Inhibition of Human Topoisomerase II by N,N,N-Trimethylethanammonium Iodide Alkylcarbazole Derivatives. *ChemMedChem* **2018**, *13*, 2635–2643. [CrossRef]
19. Caruso, A.; Ceramella, J.; Iacopetta, D.; Saturnino, C.; Mauro, M.V.; Bruno, R.; Aquaro, S.; Sinicropi, M.S. Carbazole Derivatives as Antiviral Agents: An Overview. *Molecules* **2019**, *24*, 1912. [CrossRef]
20. Giuzio, F.; Bonomo, M.G.; Catalano, A.; Infantino, V.; Salzano, G.; Monné, M.; Geronikaki, A.; Petrou, A.; Aquaro, S.; Sinicropi, M.S.; et al. Potential PDE4B inhibitors as promising candidates against SARS-CoV-2 infection. *Biomol. Concepts* **2023**, *14*, 20220033. [CrossRef]
21. Saturnino, C.; Iacopetta, D.; Sinicropi, M.S.; Rosano, C.; Caruso, A.; Caporale, A.; Marra, N.; Marengo, B.; Pronzato, M.A.; Parisi, O.I.; et al. N-alkyl carbazole derivatives as new tools for Alzheimer's disease: Preliminary studies. *Molecules* **2014**, *19*, 9307–9317. [CrossRef]
22. Saturnino, C.; Grande, F.; Aquaro, S.; Caruso, A.; Iacopetta, D.; Bonomo, M.G.; Longo, P.; Schols, D.; Sinicropi, M.S. Chloro-1,4-dimethyl-9H-carbazole Derivatives Displaying Anti-HIV Activity. *Molecules* **2018**, *23*, 286. [CrossRef]
23. Aebly, A.H.; Levy, J.N.; Steger, B.J.; Quirke, J.C.; Belitsky, J.M. Expedient synthesis of eumelanin-inspired 5,6-dihydroxyindole-2-carboxylate ethyl ester derivatives. *RSC Adv.* **2018**, *8*, 28323–28328. [CrossRef]
24. Deng, H.; Fang, Y. Synthesis and Agonistic Activity at the GPR35 of 5,6-Dihydroxyindole-2-carboxylic Acid Analogues. *ACS Med. Chem. Lett.* **2012**, *3*, 550–554. [CrossRef]
25. Luo, Z.; Jiang, Z.; Jiang, W.; Lin, D. C-H Amination of Purine Derivatives via Radical Oxidative Coupling. *J. Org. Chem.* **2018**, *83*, 3710–3718. [CrossRef]
26. Marsico, M.; Santarsiero, A.; Pappalardo, I.; Convertini, P.; Chiummiento, L.; Sardone, A.; Di Noia, M.A.; Infantino, V.; Todisco, S. Mitochondria-Mediated Apoptosis of HCC Cells Triggered by Knockdown of Glutamate Dehydrogenase 1: Perspective for Its Inhibition through Quercetin and Permethylated Anigopreissin A. *Biomedicines* **2021**, *9*, 1664. [CrossRef]
27. Su, Y.; Ding, J.; Yang, F.; He, C.; Xu, Y.; Zhu, X.; Zhou, H.; Li, H. The regulatory role of PDE4B in the progression of inflammatory function study. *Front. Pharmacol.* **2022**, *13*, 982130. [CrossRef]
28. Canton, M.; Sánchez-Rodríguez, R.; Spera, I.; Venegas, F.C.; Favia, M.; Viola, A.; Castegna, A. Reactive Oxygen Species in Macrophages: Sources and Targets. *Front. Immunol.* **2021**, *12*, 734229. [CrossRef]
29. Barua, S.; Kim, J.Y.; Yenari, M.A.; Lee, J.E. The role of NOX inhibitors in neurodegenerative diseases. *IBRO Rep.* **2019**, *7*, 59–69. [CrossRef]

30. Kaur, P.; Khan, H.; Grewal, A.K.; Dua, K.; Singh, T.G. Therapeutic potential of NOX inhibitors in neuropsychiatric disorders. *Psychopharmacology* **2023**, *240*, 1825–1840. [CrossRef]
31. Picchianti-Diamanti, A.; Spinelli, F.R.; Rosado, M.M.; Conti, F.; Laganà, B. Inhibition of Phosphodiesterase-4 in Psoriatic Arthritis and Inflammatory Bowel Diseases. *Int. J. Mol. Sci.* **2021**, *22*, 2638. [CrossRef] [PubMed]